Theory and phenomenology of coherent neutrino-nucleus scattering

Cite as: AIP Conference Proceedings **1666**, 160001 (2015); https://doi.org/10.1063/1.4915590
Published Online: 15 July 2015

Gail McLaughlin

Theory and Phenomenology of Coherent Neutrino-Nucleus Scattering

Gail McLaughlin

Department of Physics, North Carolina State University, Raleigh, NC 27695-8202

Abstract. We review the theory and phenomenology of coherent elastic neutrino-nucleus scattering (CEνNS). After a brief introduction, we summarize the places where CEνNS is already in use and then turn to future physics opportunities from CEνNS. CEνNS has been proposed as a way to limit or discover beyond the standard model physics, measure the nuclear-neutron radius and constrain the Weinberg angle.

Keywords: Neutrino, Coherent Scattering, Neutron radius
PACS: 13.13.+g, 21.10.Gv, 24.80.+y

INTRODUCTION

Coherent Elastic Neutrino Nucleus Scattering (CEνNS) is the process by which a neutrino interacts with a nucleus through the neutral current interaction and the nucleus is not excited to a higher energy state. After the collision, it is not possible to see the neutrino, but it is possible to see the small kick it gives to the nucleus.

The coherent elastic neutrino nucleus scattering cross section, assuming a spin zero nucleus and no beyond the standard model interactions is given by,

$$\frac{d\sigma}{dT}(E,T) = \frac{G_F^2}{2\pi} M \frac{Q_W^2}{4} F^2(Q^2) \times \left[2 - \frac{2T}{E} + \left(\frac{T}{E}\right)^2 - \frac{MT}{E^2}\right], \quad (1)$$

where E is the incoming neutrino energy, T is the nuclear recoil, $Q^2 = (2E^2TM)/(E^2 - ET)$ is the squared momentum transfer, $Q_W = N - Z(1 - 4\sin^2\theta_W)$ is the weak charge and F(Q^2) is the form factor. CEνNS is a neutral current interaction, so all flavors of neutrinos will participate with the same cross section. The form factor represents the largest uncertainty in the standard model cross section.

Terrestrial measurements of neutrino-nucleus coherent scattering have been discussed in the context of both reactor neutrino sources and stopped pion sources. For example the COHERENT collaboration has proposed measuring CEνNS using neutrinos produced at the Spallation Neutron Source (SNS) at ORNL [1]. The SNS produces neutrinos at a rate of 2×10^7 s^{-1} cm^2 for all flavors at a distance of 20m from the source. This flux is large enough to produce hundreds or thousands of events depending on the size of the detector [2].

These neutrinos at the SNS come from the decay at rest of pions and muons: the spectrum is shown in Fig. 1. Other possible sources of stopped pion neutrinos include include the European Spallation Source (ESS) and the J-PARC Material and Life Science Experimental Facility (MLF) [3]. Stopped pion neutrinos suitable for use with CEνNS can be produced not only by spallation sources but also by accelerators, such as DAEδALUS [4]. The Booster Neutrino Beam (BNB) has a stopped pion component very far off axis that could also be used for CEνNS [5]. Experiments using reactor neutrinos have been proposed by TEXONO [6], CONNIE at the Angra nuclear reactor, and attempted by CoGENT at the SONGS power reactor [7]. A full review of the experimental outlook for all types of neutrino sources is found elsewhere in these proceedings.

CURRENT USES FOR CEνNS

While CEνNS has never been detected experimentally, there are many contexts in which it is assumed to occur. These include supernova modeling, supernova neutrino detection, dark matter searches and sterile neutrino detection.

Supernova modelers include this process as a source of opacity for neutrinos. As discussed by O'Connor [8], it has particular relevance during the collapse phase of the pre-supernova star. During the collapse of a massive star, the core rapidly deleptonizes, becoming more neutron rich. As the neutrinos become trapped, the rate of deleptonization slows. By changing the magnitude of CEνNS, the position where the neutrinos become trapped changes. Specifically, increasing the magnitude causes the neutrinos to become trapped at higher electron fraction, while decreasing the magnitude causes the neutrinos to become trapped later, at lower electron fraction. A larger value of CEνNS then translates into a more massive core, while a smaller value means a smaller core.

XXVI International Conference on Neutrino Physics and Astrophysics
AIP Conf. Proc. 1666, 160001-1–160001-6; doi: 10.1063/1.4915590

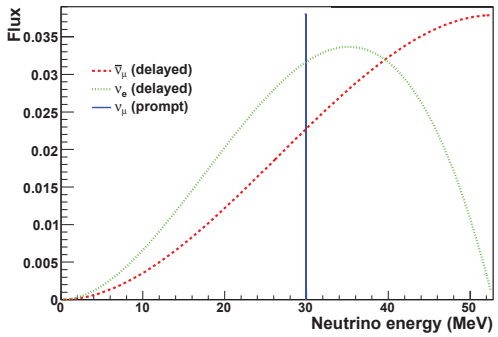

FIGURE 1. Spectrum of νs from π/μ decay at rest, Fig. from reference[2]

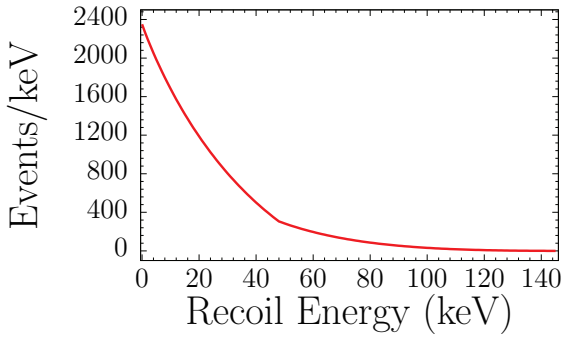

FIGURE 2. Spectrum of Argon-40 recoils from CEνNS with an incoming spectrum of neutrinos from stopped muons and pions, Fig. from reference [19].

A larger core produces a shock that proceeds further out in the star initially, but then stalls at relatively low radius. In contrast, with a smaller core, the shock proceeds more slowly at first, but doesn't stall at the same low radius. Coincident with this effect is a change in the luminosity of mu and tau type neutrinos and antineutrinos. The authors of [8] determined that a factor of two change in the cross section produces a little over 10% change in the peak luminosity of the initial mu and tau neutrinos in the supernovae.

CEνNS has been proposed as a key reaction for the measurement of supernovae neutrinos. All types of neutrinos emerge from the supernova core, and in a liquid cryogenic detector, such as CLEAN, there would be a significant number of neutral current events [9]. Worldwide, in other types of detectors, the largest numbers of events from the next galactic supernova would be charged current events, detected from the reaction $\bar{\nu}_e + p \rightarrow n + e^+$. Ideally one wishes to determine the supernova neutrino spectrum as it was originally emitted from the proto-neutron star at the center. However, flavor transformation in the form of matter enhanced flavor transformation, e.g. [10], neutrino self interaction effects, e.g. [11, 12] and parametric resonance transformations [13] will mix the spectra as the neutrinos travel out of the supernovae. Neutral current reactions are insensitive to this mixing and the rate in these reactions is determined by the sum of electron, mu and tau type neutrinos and antineutrinos. Thus they can be used in concert with charged current signals to disentangle the flavor transformation effects from the original neutrino signal as emitted at the neutrino sphere. This makes CEνNS a particularly important supernova detection mechanism

This property of CEνNS, that it is insensitive to active flavor transformation, is also ideal for studying active sterile transformation [14, 15]. Since a sterile neutrino will not interact with a nucleus through the regular weak interaction, an active sterile oscillation should show up as a decrease in the CEνNS event rate. As detailed elsewhere in these proceedings, there are a number of hints for a sterile neutrino with mass splitting $\delta m^2 \sim 1$ eV including short baseline neutrino experiments as well as reactor neutrino data. Specific proposals to use CEνNS to probe this region of parameter space include using an Argon detector with Daeδalus [14] and a monoenergetic source of neutrinos such as Argon-37 together with a cryogenic solid state bolometer [15].

In addition, CEνNS background is a limit on future dark matter sensitivity [16]. Since dark matter experiments wish to observe nucleon recoil associated with nucleus-WIMP interactions, any reaction that also produces nucleon recoils becomes a background. A recoiling nucleus from a CEνNS looks very similar to that of a WIMP interaction. As dark matter detectors look to increase their reach, they will begin to see recoils that originate from solar and atmospheric neutrinos. Without directional sensitivity this limits the interpretation of such experiments in terms of limits on the mass and cross section of WIMPs.

In order to obtain the spectrum of recoiling nuclei, one folds the incoming neutrino spectrum the cross section for the nuclei present in the detector. Typical nuclei discussed for this purpose include Argon, Germanium, Xenon, Neon, Cesium and Iodine. The recoil spectrum that one obtains when folding the stopped pion and muon spectrum with the cross section for an Argon-40 nucleus is shown in Fig. 2.

In summary, CEνNS is widely assumed to occur as predicted by the standard model. However, this process has never been detected. This is because, although the cross section is large, it is difficult to observe the small recoil of the nucleus. A first detection would be an important confirmation that this reaction exists and behaves as expected. After a first detection, however, one can begin to contemplate additional scientific opportunities.

PHYSICS OPPORTUNITIES WITH CEνNS

Several ideas have been put forward that use CEνNS to increase our understanding of particle and nuclear physics. These include limits on a detection of non-standard ν interactions, a determination of the nuclear-neutron form factor, detection of the axial part of cross section (for spin non-zero cross section), measurement of $\sin^2\theta_W$, and detection of or limits on a beyond the standard model neutrino magnetic moment.

Non-standard interactions

Limits on beyond the standard model particle physics, is an area in which CEνNS can contribute. Some non-standard interactions are currently poorly constrained but can be probed relatively easily with CEνNS. Examples are vector couplings for electron neutrinos with up and down quarks, ε_{ee}^{uV} and ε_{ee}^{dV}, although there are other couplings that contribute as well. To illustrate, we first define the non standard interactions (NSI) as follows [17],

$$\mathscr{L}_{\nu Hadron}^{NSI} = -\frac{G_F}{\sqrt{2}} \sum_{\substack{q=u,d \\ \alpha,\beta=e,\mu,\tau}} \left[\bar{\nu}_\alpha \gamma^\mu (1-\gamma^5)\nu_\beta\right] \qquad (2)$$
$$\times \left(\varepsilon_{\alpha\beta}^{qL}\left[\bar{q}\gamma_\mu(1-\gamma^5)q\right] + \varepsilon_{\alpha\beta}^{qR}\left[\bar{q}\gamma_\mu(1+\gamma^5)q\right]\right).$$

The vector couplings are the ones relevant for spin zero nuclei: $\varepsilon_{\alpha\beta}^{qV} = \varepsilon_{\alpha\beta}^{qL} + \varepsilon_{\alpha\beta}^{qR}$. These quantities are not tightly constrained. Current limits on the vector couplings are $-1.0 < \varepsilon_{ee}^{uV} < 0.6$ and $-0.5 < \varepsilon_{ee}^{dV} < 1.2$. Since these non standard interactions may be as large as the standard model weak interaction, they can be expected to have a significant effect on the CEνNS.

The new couplings are in principle incorporated into the full expression for the cross section, and change the overall form factor. However, one can make a reasonable estimate by looking a the zero order effect, which can be seen by simply changing the weak charge, Q_W,

$$\begin{aligned} Q_W &= N(1-2\varepsilon_{ee}^{uV} - 4\varepsilon_{ee}^{dV}) \qquad (3) \\ &\quad + Z(1-4\sin^2\theta_W + 4\varepsilon_{ee}^{uV} + 2\varepsilon_{ee}^{dV}). \end{aligned}$$

From Eq. 1 we see that this change in Q_W adjusts the overall magnitude of the cross section, which translates in the a shift in the overall magnitude of the nuclear recoil curve. In Fig. 3, the limits on these non-standard interactions that could be achieved with 100kg of Ne in one year, using neutrinos from the Spallation Neutron Source (SNS) at ORNL. As can be seen from the figure, there is substantial improvement in the current limits for even this moderate amount of target material.

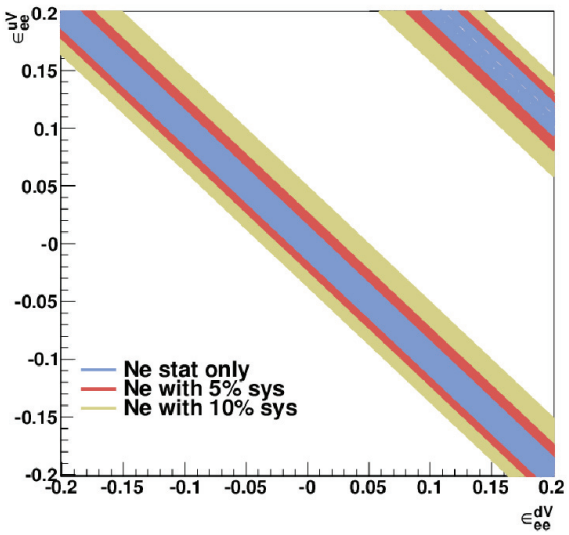

FIGURE 3. Shows the allowed region at 90% confidence of the vector couplings for 100 kg/yr of ^{20}Ne at the SNS. The regions show systematic uncertainty of 0, 5% and 20% in addition to statistical uncertainty. Fig. from [2].

Additional non-standard interactions such as the flavor changing neutral currents will also influence the nuclear recoil curve. Limits on non-standard interactions need to be carefully interpreted since if one considers all possible channels, then the limit is placed on a combination of unknown couplings. Nevertheless, since there are many channels in which the non-standard interaction is poorly constrained, one can expect improved limits using CEνNS.

Form Factor

CEνNS can also make a contribution to nuclear structure physics, through an improved understanding of the distribution of neutrons inside the nucleus. This distribution is can be determined through a measurement of the form factor.

The form factor from Eq. 1, $F(Q^2)$ is the Fourier transform of the density distributions of protons and neutrons in the nucleus.

$$\begin{aligned} F(Q^2) &= \frac{1}{Q_W}\int r^2 dr \frac{\sin(Qr)}{Qr} \qquad (4) \\ &\quad \times \left[\rho_n(r) - (1-4\sin^2\theta_W)\rho_p(r)\right]. \end{aligned}$$

Here ρ_n and ρ_p are the density distributions of neutrons and protons respectively and Eq. 4 assumes a spherical nucleus. In Fig. 4 the neutron density, $\rho_n(r)$ as a function of nuclear radius is shown for two different Skyrme functionals. A measure of the overall size of the neutron

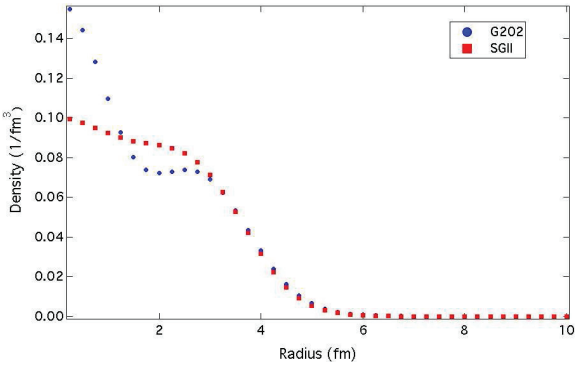

FIGURE 4. Shows the density distribution in a spherical nucleus as calculated with the Skyrme forces SGII and G202, Fig. from [19]

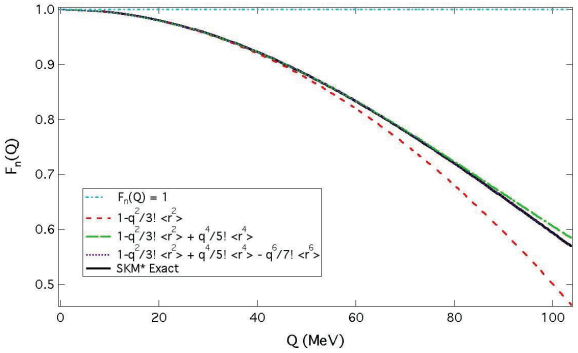

FIGURE 5. The neutron form factors $F_n(Q^2)$ for 40Ar predicted by the Skyrme functional SkMâĹŮ (solid black curve), and truncations of the expanded form factor at various orders of Q: Q^0 (dotted blue curve), Q^2 (dashed red curve), Q^4 (dot-dashed green curve), and, in the bottom panel, Q^6 (dotted purple curve). [19]

distribution in the nucleus is the "neutron radius" which is defined as

$$\langle R_n^2\rangle^{1/2} = \frac{1}{N}\left[\int \left(\rho_n r^2\right) r^2 dr\right]^{1/2} \tag{5}$$

The neutron radii for the curves in Fig. 4 are $\langle R_n^2\rangle^{1/2}_{SGII}$ = 3.405 fm and $\langle R_n^2\rangle^{1/2}_{G202}$ = 3.454 fm.

Proton form factors, i.e. the part of Eq. 4 that depends on ρ_p, can be determined by electromagnetic probes and so can therefore can be considered reasonably well known. However, by examining Eq. 4 we see that the proton form factor is suppressed by the prefactor $1 - 4\sin^2\theta_W$. Therefore the proton form factor plays a small role in determining the CEνNS cross section.

The neutron form factor, which is not similarly suppressed, is less well constrained by experiment. Traditionally the neutron form factor has been been probed using hadronic methods, for example neutron scattering. Because it is a hadronic probe, interpreting these experiments in terms of the distribution of neutrons in the nucleus requires a theoretical model to extract the neutron radius from the cross section. Typical quoted errors on the neutron radius are between 1% and 10%. Another avenue is parity violating electron scattering. The PREX experiment [20], as well as CREX, at JLab are polarized electron scattering experiments, where it is the the difference between the two polarizations from which the parity violating asymmetry A_{PV} is extracted. The PREX measurement on lead gives $A_{PV} \sim 0.65 \times 10^{-6}$, which is then interpreted in terms of neutron radius.

These leaves open the possibility that CEνNS can be used as a complementary method to determine the form factor [18]. To determine the form factor using CEνNS, the nuclear recoil curve can be fit to two or three parameters, the neutron radius and higher moments, independent of a nuclear model. This happens because the $\sin(Qr)$ in the form factor can be expanded as

$$\begin{aligned} F_n(Q^2) &= \frac{1}{Q_W}\int \rho_n(r)\frac{\sin(Qr)}{Qr} r^2 dr \\ &\approx \frac{N}{Q_W}\left(1 - \frac{Q^2}{3!}\langle R_n^2\rangle + \frac{Q^4}{5!}\langle R_n^4\rangle - \ldots\right). \end{aligned} \tag{6}$$

The form factor is now written in terms of moments of the density distribution. The first term is the zeroth order cross section which is a good approximation if the incoming neutrino energies are sufficiently low, so that the nucleus can be treated as a point particle. Neutrinos from reactors are in this category.

The size of the form factor as a function of Q^2 is shown in Fig. 5. At low momentum transfer the form factor approaches unity. At higher momentum transfer the form factor is reduced and additional terms in the expansion are needed to properly characterize it. These next terms take account of the finite size of the nucleus. The second term, $\langle R_n^2\rangle$, is the neutron radius, and the third term, $\langle R_n^4\rangle$ is the fourth moment. These two moments are sufficient to characterize the form factor with energies of pion and muon decay at rest neutrinos [19].

One can evaluate how well the first two moments can be constrained by looking at a couple of scenarios with different target materials. In Fig. 6, we show the results for a Monte Carlo with liquid argon. The incoming neutrino flux corresponds to 3.5 tonnes argon 16m from SNS, 18m from Daeδalus, 30m from ESS for one year. One can see that not only would it be possible to address the discrepancy between the theory calculations and the previous of measurement, it would be also be possible to make a first measurement of the fourth moment of the density distribution.

Another possible target material is xenon. Xenon has more nucleons, and as a result the form factor correction

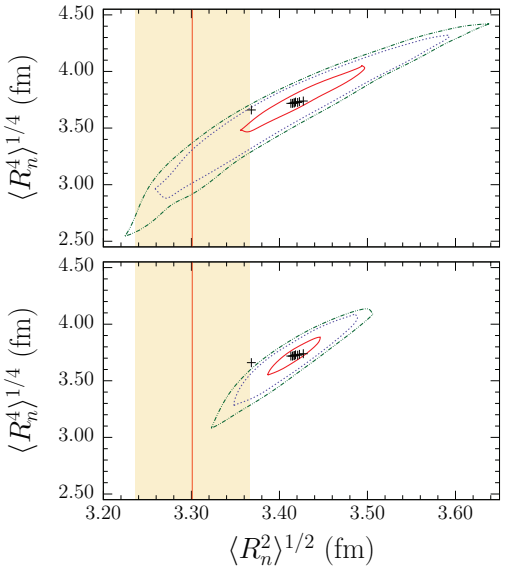

FIGURE 6. Shows 40%, 91% and 97% confidence contours. Crosses are theory predictions. Band is measurement from neutron scattering. Top plot: normalization of neutrino flux not known, bottom plot normalization of neutrino flux known. Fig. from [19].

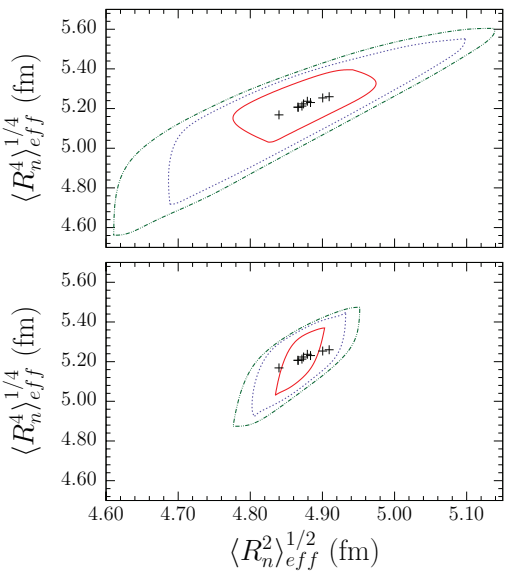

FIGURE 7. 300 kg Xenon Shows 40%, 91% and 97% confidence contours. Crosses are theory predictions. Fig. from [19]

is larger. In Fig. 7, the incoming neutrino flux is equivalent to placing 300 kg Xenon 16m from SNS, 18m from Daeδalus, 30m from ESS for one year. As can be seen from the figure, considerably less xenon is require to obtain the same precision on the neutron radius.

Weinberg angle

The Weinberg angle is the second largest uncertainty in the cross section (Eq. 1). Similar to the case of the non standard interactions, the primary effect of the uncertainty in the Weinberg angle is a change in Q_W which adjust the overall value of the cross section, and therefore the overall magnitude of the recoil curve. There are more stringent constraints on the Weinberg angle than on nonstandard neutrino interactions, but CEνNS again provides a complementary approach to constraining this quantity. The better the overall magnitude of the incoming neutrino flux can be constrained, the more stringent the limit on the Weinberg angle can become.

Neutrino magnetic moment

The neutrino magnetic moment adds a term to the CEνNS cross section that produces an upturn in the the recoil spectrum at low recoil energy. For a magnetic moment of order $\mu_\nu \sim 10^{-10}$ the recoil curve begins to deviate from the no-magnetic moment one at recoils in the eV range. Thus, this measurement requires a low threshold.

CONCLUSIONS

Coherent elastic neutrino nucleus scattering has not yet been detected, but in many communities such as supernova simulation, supernova detection, active-sterile oscillations, and dark matter detection it is assumed to exist as predicted by the standard model. A first detection would be an important confirmation that this process is being taken into account properly in these areas. Beyond a first detection there are a number of scientific avenues that can be explored. These include improved limits on nonstandard neutrino interactions, an independent probe of nuclear-neutron form factors, and complementary limits on the Weinberg angle. With sufficiently low threshold, the neutrino magnetic moment can be explored as well. Overall CEνNS presents interesting opportunity from the theoretical and phenomenological point of view.

ACKNOWLEDGMENTS

We thank Kate Scholberg and Phil Barbeau for useful discussions. This contribution was supported by US DOE Contract No. DE-FG02-02ER41216

REFERENCES

1. Adam et al, “COHERENT at the Spallation Neutron Source”, a position paper, http://fsnutown.phy.ornl.gov/fsnufiles /positionpapers/Coherent_PositionPaper.pdf
2. K. Scholberg, Phys. Rev. D **73**, 033005 (2006) [hep-ex/0511042].
3. Y. Ikeda, "1 MW Pulse Spallation Neutron Source (JSNS) under the High Intensity Proton Accelerator Project", Proceedings of ICANS-XVI, 16th Meeting of the International Collaboration on Advanced Neutron Sources, 2003.
4. Alonso, J. et al., "Expression of Interest for a Novel Search for CP Violation in the Neutrino Sector: DAEδALUS”, arXiv 1006.0260, 2010.
5. Yoo, J., "Measuring coherent-NCνAs at Fermilab", http://if-neutrino.fnal.gov/ne utrino1-pagers.pdf, 2011
6. Henry T. Wong *et al.*, J. Phys. Conf. Ser. **39**, 266 (2006), hep-ex/0511001, TAUP-2005 Workshop, Spain, 2005.
7. P. S. Barbeau, J. I. Collar, and O. Tench ., JCAP, 2007(09):009, 2007
8. E. O’Connor et al, in preparation (2014)
9. C. J. Horowitz, K. L. Coakley, and D. N. McKinsey, *Phys. Rev.* **D**68 0203005 (2003) .
10. C. Lunardini and A. Y. Smirnov, JCAP **0306**, 009 (2003) [hep-ph/0302033].
11. H. Duan, G. M. Fuller and Y. Z. Qian, Phys. Rev. D **74**, 123004 (2006) [astro-ph/0511275].
12. Y. Pehlivan, A. B. Balantekin, T. Kajino and T. Yoshida, Phys. Rev. D **84**, 065008 (2011) [arXiv:1105.1182 [astro-ph.CO]].
13. K. M. Patton, J. P. Kneller and G. C. McLaughlin, arXiv:1407.7835 [hep-ph].
14. A. J. Anderson, J. M. Conrad, E. Figueroa-Feliciano, C. Ignarra, G. Karagiorgi, K. Scholberg, M. H. Shaevitz and J. Spitz, Phys. Rev. D **86** (2012) 013004 [arXiv:1201.3805 [hep-ph]].
15. J. A. Formaggio, E. Figueroa-Feliciano and A. J. Anderson, Phys. Rev. D **85** (2012) 013009 [arXiv:1107.3512 [hep-ph]].
16. J. Billard, L. Strigari and E. Figueroa-Feliciano, Phys. Rev. D **89**, 023524 (2014) [arXiv:1307.5458 [hep-ph]].
17. J. Barranco, O. G. Miranda and T. I. Rashba, JHEP **0512**, 021 (2005) [hep-ph/0508299].
18. P. S. Amanik and G. C. McLaughlin, *J. Phys. G* **3**6, 015105 (2009).
19. K. Patton, J. Engel, G. C. McLaughlin and N. Schunck, *Phys. Rev.* **8**5, 024612 (2012) [arXiv:1207.0693 [nucl-th]].
20. S. Abrahamyan et al. (PREX Collaboration), Phys. Rev. Lett. 108, 112502 (2012).
21. K. M. Patton, G. C. McLaughlin and K. Scholberg, *Int. J. Mod. Phys.* **2**2, 1330013 (2013).
22. D. Akimov *et al.* [CSI Collaboration], arXiv:1310.0125 [hep-ex].